

Structures and Properties of Mixed DNA Bases Tetrads: Nonempirical *ab Initio* HF and DFT Studies

Jiande Gu[†] and Jerzy Leszczynski^{*‡}

State Key Laboratory of Drug Research, Shanghai Institute of Materia Medica, Chinese Academy of Sciences, Shanghai 200031, P. R. China, and The Computational Center of Molecular Structure and Interactions, Department of Chemistry, Jackson State University, Jackson, Mississippi 39217

Received: August 20, 1999; In Final Form: November 15, 1999

Three nonplanar tetrads of the DNA bases (Watson–Crick-type TATA, Hoogsteen-type TATA, and AGAG tetrad) are studied at the HF/6-311G(d,p) and B3LYP/6-311G(d,p) levels of theory. Both Hoogsteen and Watson–Crick type thymine–adenine–thymine–adenine tetrads are stable in the isolated form in which the Hoogsteen type TATA tetrad is about 2.3 kcal/mol more stable than the Watson–Crick type. The significant stabilization energies of over 30 kcal/mol predicted for the TATA tetrads confirm that the stabilization of this structure plays a key role in the four stranded helices. The energy of each bifurcated H-bond in the tetrads has been found to be about 8 kcal/mol for the planar structure and about 3 kcal/mol for the nonplanar tetrad. The formation of bifurcated H-bonding is the main contribution to the creation of the tetrad structure. The electrostatic potential map suggests that the presence of a cation in the system is expected to further stabilize the TATA tetrad in both forms. However, metal ions are unlikely to be stable in the center of the TATA tetrads. The V-shape structure of the AGAG tetrad and 3.5 kcal/mol of stabilizing energy (compared to the two separated AG pair) revealed in this study suggest that this tetrad structure may not be important in the tetraplexes.

Introduction

Four-stranded DNA structures, formed upon H-bonding interactions between two DNA duplexes, have been considered to provide possible models for DNA strand exchange processes.^{1,2} H-bonding patterns between two nucleobases have been observed in guanine tetrads,^{3–5} thymine tetrad,⁶ and also in RNA, uracil tetrads.⁷ Recent quantum chemical study of the guanine tetrad suggests that the bifurcated hydrogen bonding of the O6 atom of guanine with the hydrogen attached to the N1 and the hydrogen from the amino group of the other guanine unite plays a central role in stabilizing the guanine tetrad in the absence of cation interactions.⁸ This kind of H-bonding pattern has also been found between guanine and cytosine.^{9–11} There are a number of possible structures which could be derived for the thymine and adenine formed tetrads. Among the various types of tetrads that are expected from the considerations of symmetry, the two which contain the bifurcated hydrogen bonds are the most important in stabilizing the poly(dT)•poly(dA)•poly(dA)•poly(dT) tetraplexes.¹² Chemical probing studies of d(G3TTAG3) and d(TTAG3) units of different lengths suggest that N7 of adenine is inaccessible, signifying the possibility of the formation of AGAG tetrad in the tetraplexes.^{13,14} However, some studies question the existence of the AGAG tetrad because it has relatively higher energy and lacks the tetrad of oxygen required for the formation of the cation site.^{14,15} To reveal the nature and function of the bifurcated hydrogen bonds in the tetraplexes, much attention needs to be paid to investigations of molecular structures and bonding patterns of various tetrads. Although the structure and stability of tetraplexes does not solely

depend on the interaction of isolated tetrads of the bases, the base pairing might be the crucial factors in the formation of tetraplexes. Details of the interactions and the base pairing could only be explored by accurate computational studies.

In this paper, we report the first *ab initio* quantum chemistry study of the stability and structure of three nonplanar tetrads: Watson–Crick-type TATA and Hoogsteen-type TATA and AGAG tetrads (Figures 1, 2, and 8). Because of the relatively large size of such systems, no theoretical investigations of the energy minimum structure of these tetrads based on the reliable *ab initio* quantum chemistry methods have been reported so far. The aim of our study is to reveal the details of the molecular geometries, the energy properties, and the electrostatic potential characteristics involved in the formation of these nonplanar tetrads.

Method of Calculation

The local minima of the three tetrad structures have been fully optimized by the analytic gradient techniques using the density functional theory with Becke's three-parameter (B3)¹⁶ exchange functional along with the Lee–Yang–Parr (LYP) nonlocal correlation functional^{17,18} (B3LYP). The standard valence triple- ζ basis set augmented with six d-type and three p-type polarization functions, 6-311G(d,p),¹⁹ was used in conjunction with the DFT method. In the comprehensive investigations, Mebel, Morokuma, and Lin²⁰ demonstrated that the geometries and frequencies of the molecules calculated at the B3LYP/6-311G(d,p) level agree well with experiment. The absolute deviations for the bond lengths and angles at the B3LYP/6-311G(d,p) level are smaller than those at the *ab initio* MP2/6-31G(d) and QCISD/6-31G(d) levels of theory.²¹ Our previous studies of hydrogen bonded systems involving DNA

* Corresponding author.

[†] Chinese Academy of Sciences.

[‡] Jackson State University.

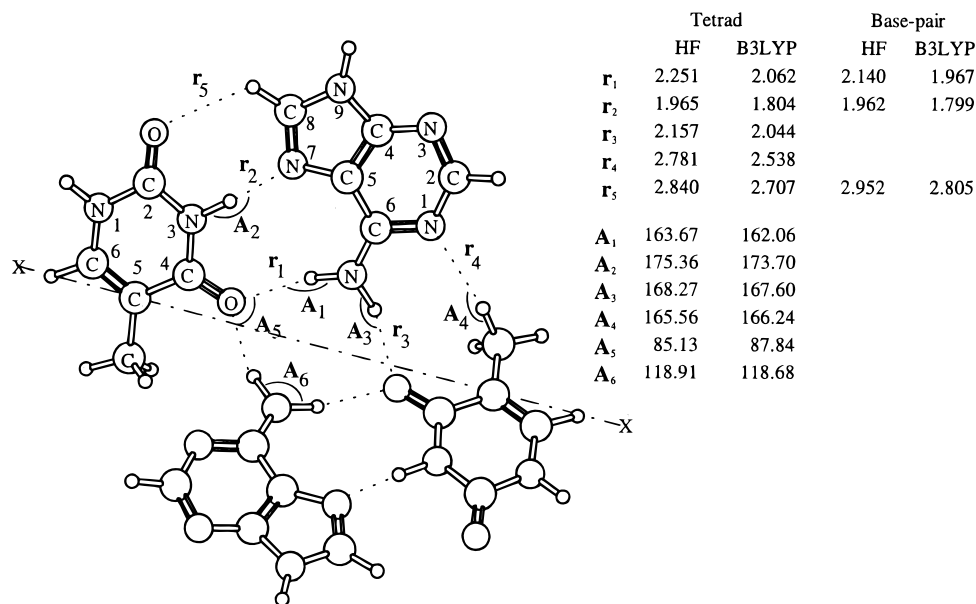


Figure 1. Fully optimized Hoogsteen type thymine-adenine-thymine-adenine tetrad (TATAH) structure. Atomic distances in angstroms and angles in degrees. X- -X is the folding line. Base pair parameters are also listed for comparison. Basis set used in all the calculation is 6-311G(d,p).

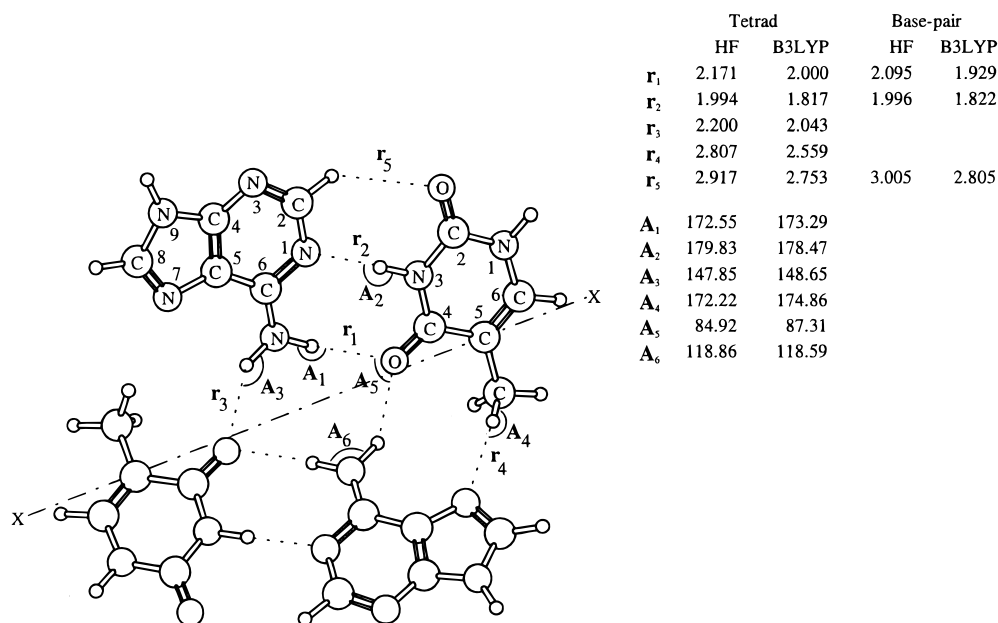


Figure 2. Fully optimized Watson-Crick type thymine-adenine-thymine-adenine tetrad (TATAW) structure. Atomic distances in angstroms and angles in degrees. X- -X is the folding line. Base pair parameters are also listed for comparison. Basis set used in all the calculation is 6-311G(d,p).

bases have shown that the B3LYP approach predicts reliable interaction energies and is compatible to the MP2/6-31(d,p) method.^{22,23} Also, the performance of HF approximation was examined in this study because it is cheaper than the B3LYP method and it predicts similar stabilization energy for the G-tetrad as shown in our guanine-tetrad calculations.⁸ This suggests that for larger H-bonded systems which are too large to apply electron correlated approaches the HF/6-311G(d,p) level of theory could be a cost-effective method for the evaluation of their bonding characteristics. The Gaussian-94 package of programs²⁴ was used in the calculations.

Results and Discussion

TATA Tetrads. As revealed by calculations, there are similarities between the Watson-Crick and Hoogsteen AT pairs.

Both are characterized by bifurcated hydrogen bonding between the O4 of thymine and the protons of the amino groups of adenines not involved in the AT pair bonds. Thus, each thymine is simultaneously bonded to two adenines and each adenine to two thymines. No significant geometric change has been observed inside the bases when the tetrads are formed. The optimized energy minimal structures of these two tetrads are depicted in Figures 1 and 2. The AT pair itself is almost in one plane for both of the Watson-Crick and Hoogsteen systems as can be seen in Figure 3. However, in the tetrad, two Hoogsteen AT pairs are tilted at 138° relative to each other along the folding line between the two C5 atoms of the thymines. This folding angle amounts to 139° in the Watson-Crick pairs tetrad. The optimized structures of the TATA tetrads indicate the existence of six strong hydrogen bonds in the system. The lengths of two

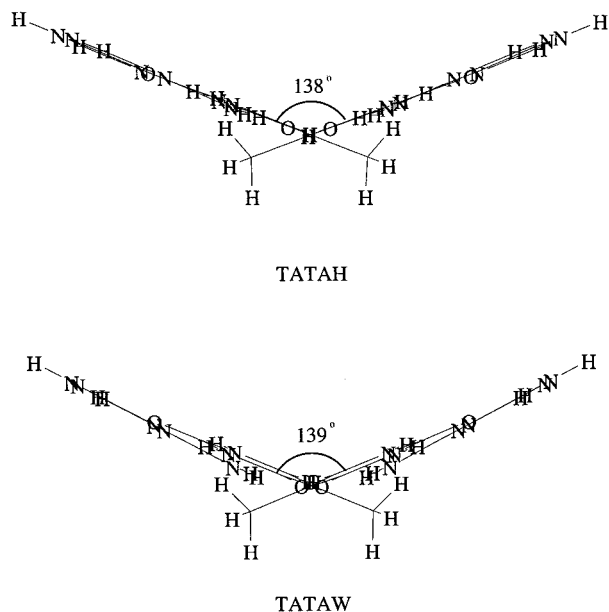


Figure 3. Folding of the AT pairs in the tetrads where the folding lines are perpendicular to the paper. The AT pairs in TATAW are slightly twisted.

H-bonds in each Hoogsteen AT pair are 1.80 (N7(A)···H3(T)) and 2.06 Å (O4(T)···H6(A)), respectively. These two corresponding bond distances are 1.82 and 2.00 Å in the Watson–Crick pairs. The O4···H bonding in the Watson–Crick pairs is slightly shorter than that in the Hoogsteen type tetrad. On the other hand, the H-bonds linking the two AT pairs of the tetrad are about 0.03 Å shorter in the Hoogsteen type tetrad than those in the Watson–Crick type. In addition to the hydrogen bonds mentioned above, there is one more pair of weak H-bonding between N1 of adenine and H in the methyl group of thymine (2.54 Å) in the Hoogsteen type tetrad and between N7 of adenine and the methyl H of thymine (2.56 Å) in the Watson–Crick. Although these H-bonds are weaker, they play the main role in governing the nonplanar geometry of the tetrads. The AT pairs in the tetrads are folded to adopt a conformation which favors this weak bonding. This is manifested by the similar folding angles in the different TATA tetrads. In Figures 1 and 2, the main geometric parameters of AT base pairs are also listed. It is clear that the AT base pairs do not experience significant changes inside the tetrads.

The energy characteristics of the TATA tetrads are listed in Table 1. The total energy of the Hoogsteen type TATA tetrad is about 2.3 kcal/mol lower than the energy of the Watson–Crick type. The stabilization energy relative to the isolated bases of the tetrads is 32.7 kcal/mol for the former and 30.4 kcal/mol for the latter. This amounts to about only half of the stabilization energy predicted for the guanine-tetrad (66.5 kcal/mol after the BSSE²⁵ correction). There are eight strong H-bonds in the planar G-tetrad. The significant difference of the stabilization energy between the nonplanar TATA tetrads and the planar G-tetrad suggests that the nonplanar bifurcated H-bonding is weaker. This can be attributed to the orientational preference of the H-bonding. The energy difference between the tetrads and the two AT base pairs is 7.6 kcal/mol in the Hoogsteen type TATA tetrad and 6.6 kcal/mol in the Watson–Crick type tetrad. By rotating the methyl group along the C5–C_{methyl} bond in thymine, we estimate that the energy of the N1(A)···H(T) H-bonding (r4 in Figures 1 and 2) is about 1.6 kcal/mol. This indicates that a decrease in stabilization due to the unfavored direction of H-bonding in the bifurcated pattern amounts to about 5 kcal/

TABLE 1: Energy Properties of the Bases, Base Pairs, and Base Tetrads Calculated at the B3LYP/6-311G(d,p) and HF/6-311G(d,p) Levels (Bold)

	<i>E</i> (hartree)	BSSE (kcal/mol)	ΔE^a (kcal/mol)	ΔE^{BSSE^b} (kcal/mol)	$\Delta E(I)^{BSSE^c}$ (kcal/mol)
Bases					
guanine	-542.6979127	-3.02 ^d -2.41 ^f			
	-539.5275126	-1.82^d -1.61^f			
adenine	-467.4392151	-1.89 ^d -2.28 ^e			
	-464.6291433	-1.26^d -1.36^e			
thymine	-454.2646891	-2.74 ^e -1.63^e			
Base Pairs					
ATH	-921.728883	-1.86	-15.68 ^g		-12.52
	-916.271366	-1.14	-11.73^g		-9.88
ATW	-921.727955	-1.85	-15.09 ^g		-11.92
	-916.270400	-1.11	-11.12^g		-9.24
AG	-1010.162940	-1.66	-16.20 ^g		-12.95
	-1004.175515	-1.01	-11.83^g		-9.76
Tetrads					
GGGG	-2170.9129674		-76.13	-66.49	
	-2158.2195132		-68.72	-62.28	
AGAG	-2020.3367716		-39.23	-29.41	-3.51
	-2008.3597579		-32.13	-25.97	-2.39
TATAH	-1843.4758559		-42.70	-32.66	-7.63
	-1832.5558529		-31.63	-25.65	-5.95
TATAW	-1843.4722645		-40.45	-30.43	-6.56
	-1832.5523047		-29.46	-23.48	-5.00

^a $\Delta E = E(\text{tetrad}) - 2E(\text{base1}) - 2E(\text{base2})$. ^b $\Delta E^{BSSE} = \Delta E - 2BSSE(\text{base1}) - 2BSSE(\text{base2})$ for the tetrad and $\Delta E - BSSE(\text{base1}) - BSSE(\text{base2})$ for the base pair. ^c $\Delta E(I)^{BSSE} = E(\text{tetrad}) - 2E(\text{base pair}) - 2BSSE(\text{base pair})$. ^d Calculated in AGAG tetrad. ^e Calculated in ATATH and ATATW tetrads. ^f Calculated in G-tetrad. ^g $\Delta E = E(\text{base-pair}) - E(\text{base1}) - E(\text{base2})$.

mol. As a comparison, the bonding energy of each H-bond in the G-tetrad with eight hydrogen bonds amounts to 8.6 kcal/mol. In the stability study of poly(dT)·poly(dA)·poly(dA)·poly(dT) tetraplexes, the Hoogsteen type TATA has been found to be stabilized by 21.8 kcal/mol, while the Watson–Crick type tetrad is stabilized by 20.0 kcal/mol.¹² The predicted stabilization energies for these systems of 32.7 and 30.4 kcal/mol confirm that the stabilization of the tetrads plays a key role in the formation of the four stranded helices.

It is interesting to compare the details of the H-bonds in tetrads with those in base pairs. For the Hoogsteen type, the O4(T)···H6(A) distance of 2.06 Å is about 0.1 Å longer in the tetrad than in the base pair (1.97 Å). However, the O2(T)···H8(A) atomic distance decreases by about 0.1 Å in the tetrad, while H3(T)···N7(A) bond length is virtually unchanged. The same changes can be seen in the Watson–Crick type tetrad. These changes imply that the formation of the second set of H-bond in the bifurcated hydrogen bonds weakens slightly the existent H-bonds of the base pairs. According to the O2(T)···H8(A) atomic distance of 2.7 Å in the tetrad, it is unlikely that the O2(T)···H8(A) interaction is of importance in the formation of the tetrads. The energy difference of 2.3 kcal/mol between the two tetrads is partly due to the energy difference between the WC AT base pair and the Hoogsteen AT base pair which amounts to 1.2 kcal/mol. The other 1.1 kcal/mol is clearly from the difference between the interactions of the base pairs. Since the r4 type H-bonds are basically the same in both tetrads, the less linear r3 type H-bonds in the WC TATA tetrad result in lower stabilization energy.

The electrostatic potential (ESP) map provides a simple way to predict how different geometries could alter the reactivities

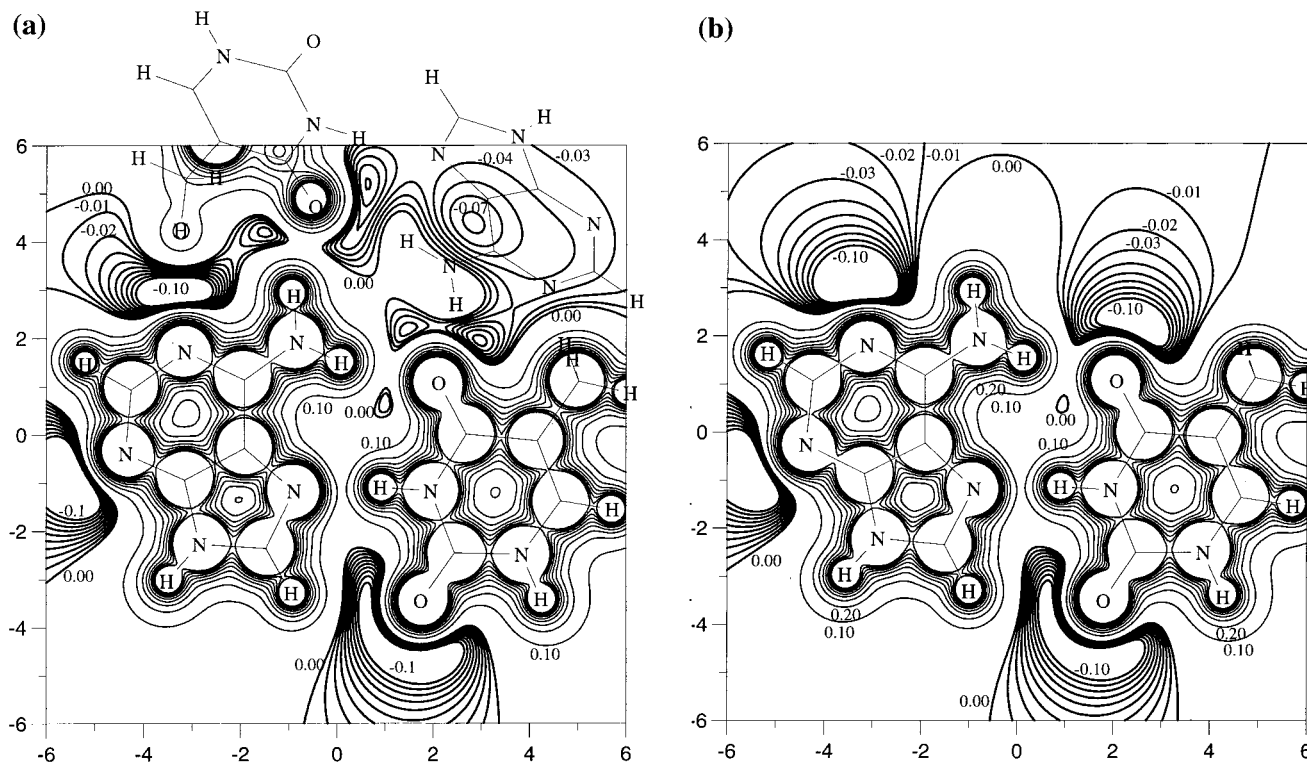


Figure 4. Electrostatic potential map of TATAH (a) and AT base pair (b). The plane of the AT base pair. The thin line represents the positive part of electrostatic potential, and the thick line is the negative parts of electrostatic potential. The contour spacing is 0.1 au for the positive part and 0.01 au for the negative part. The unit of the axes is angstroms.

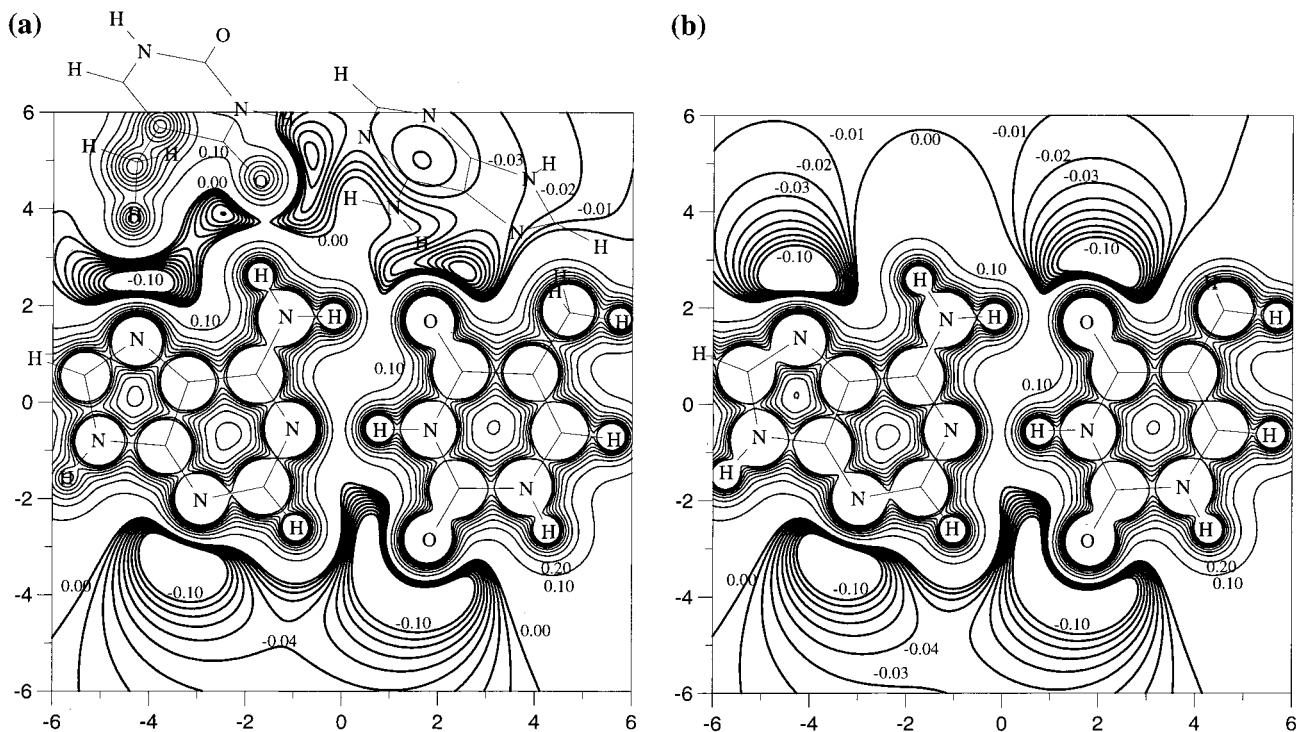


Figure 5. Electrostatic potential map of TATAW (a) and AT base pair (b). The plane of the AT base pair. The thin line represents the positive part of electrostatic potential, and the thick line is the negative parts of the electrostatic potential. The contour spacing is 0.1 au for the positive part and 0.01 au for the negative part. The unit of the axes is in angstroms.

in intact DNA. It can also be used to identify the possible metal interaction sites. Figure 4 displays the electrostatic potential of the Hoogsteen TATA plotted on one of the AT pairs plane. For comparison, the ESP map of the Hoogsteen AT base pairs is also shown in Figure 4. The ESP maps of the Watson–Crick TATA tetrad and its AT base pair are depicted in Figure 5.

The formation of the tetrads can be viewed as the binding between the two AT pairs as shown in the figures. The main change occurring in going from the AT base pair to the tetrad can be seen in the bifurcated H-bonding area. The ESP related to the other parts of the systems is virtually unchanged as the pairs form the tetrads. The negative electrostatic potential area

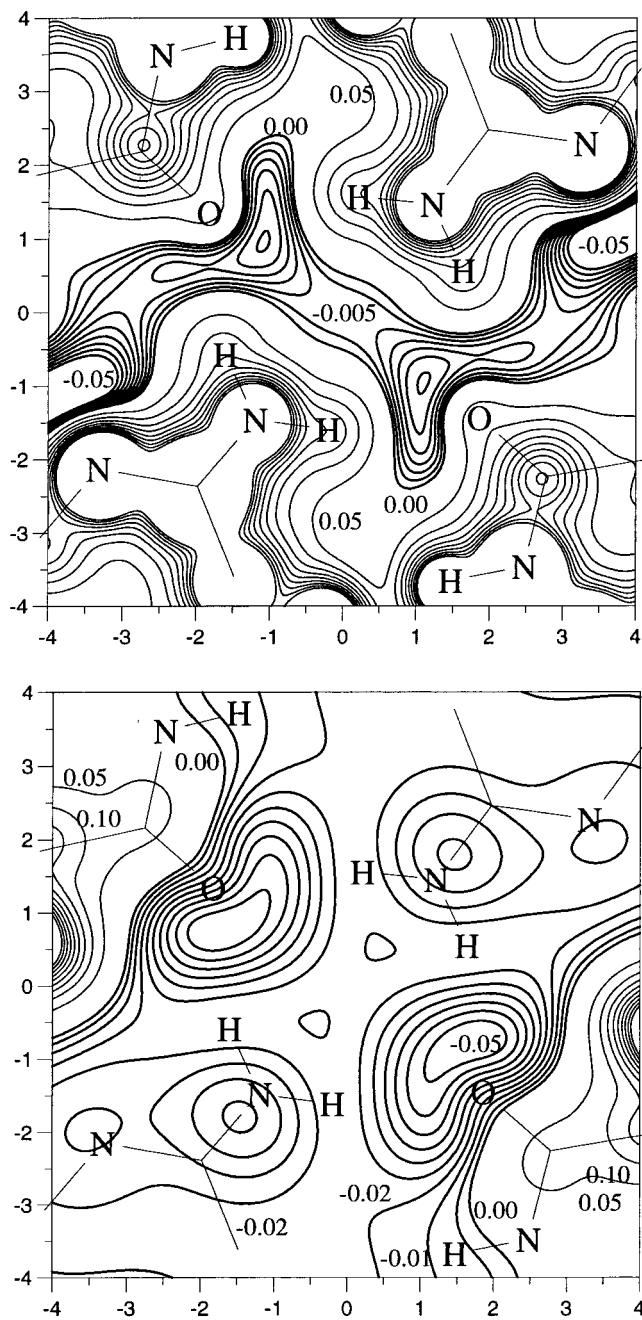


Figure 6. Electrostatic potential map of the central area of TATAH. The top panel is the ESP on the central plane of N6O4N6'O4' atoms. The bottom panel is the ESP 1.2 Å above the central plane. The thin line represents the positive part of electrostatic potential, and the thick line is the negative parts of electrostatic potential. The contour spacing is 0.05 au for the positive part and 0.005 au for the negative part. The unit of the axes is angstroms.

above O4–O4' in the maps suggests the potential cation hosting position for the tetrads. Figures 6 and 7 show the ESPs of the central area of both TATA tetrads. The center of the tetrads has a small negative electrostatic potential area due to the presence of the H-bonded hydrogen atoms. The influence of the hydrogen atoms becomes less important in the area above the center of the tetrads as shown in the figures. The presence of a cation such as Na⁺, K⁺, and NH₄⁺ in the system is expected to further stabilize the TATA tetrad in both forms when the cation is located above the central area. However, unlike the guanine tetrad in which a cation (Na⁺) can be host in the center of the tetrad,^{3–5} metal ions are unlikely to be stable in the center

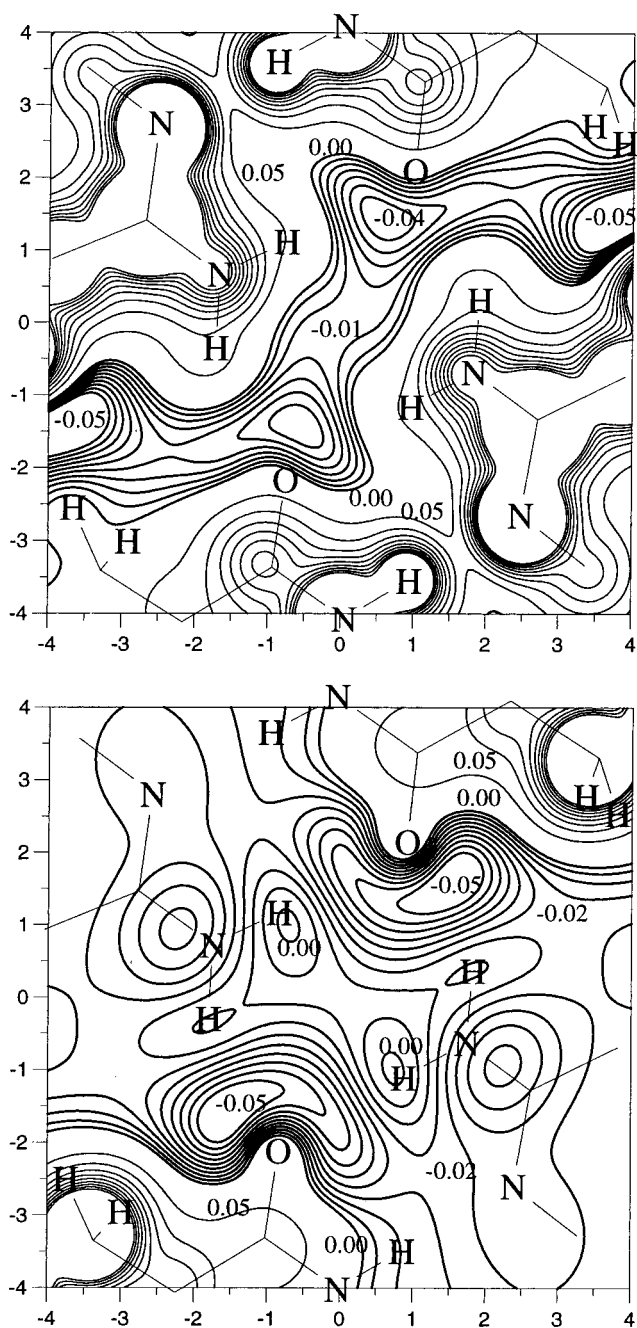


Figure 7. Electrostatic potential map of the central area of TATAW. The top panel is the ESP on the central plane of N6O4N6'O4' atoms. The bottom panel is the ESP 1.2 Å above the central plane. The thin line represents the positive part of electrostatic potential, and the thick line is the negative parts of electrostatic potential. The contour spacing is 0.05 au for the positive part and 0.005 au for the negative part. The unit of the axes is in angstroms.

of the TATA tetrads because of the influence of the H bonded hydrogen atoms.

AGAG Tetrad. The geometries of the bases are basically unchanged during the formation of the AGAG tetrad. The details of the geometry of the energy-minimum structure of AGAG show that this tetrad is formed by two AG pairs through two weak hydrogen bonds in between. Each AG pair is strongly bonded with the binding energy of 16.2 (13.0 after BSSE) kcal/mol. There are some interesting geometrical features of this structure. First, the AG pairs in the tetrad are not planar as can be seen from the figure. Two guanines are tilted by an angle of 92° along the N7–N7' axis, while two adenines are folded at

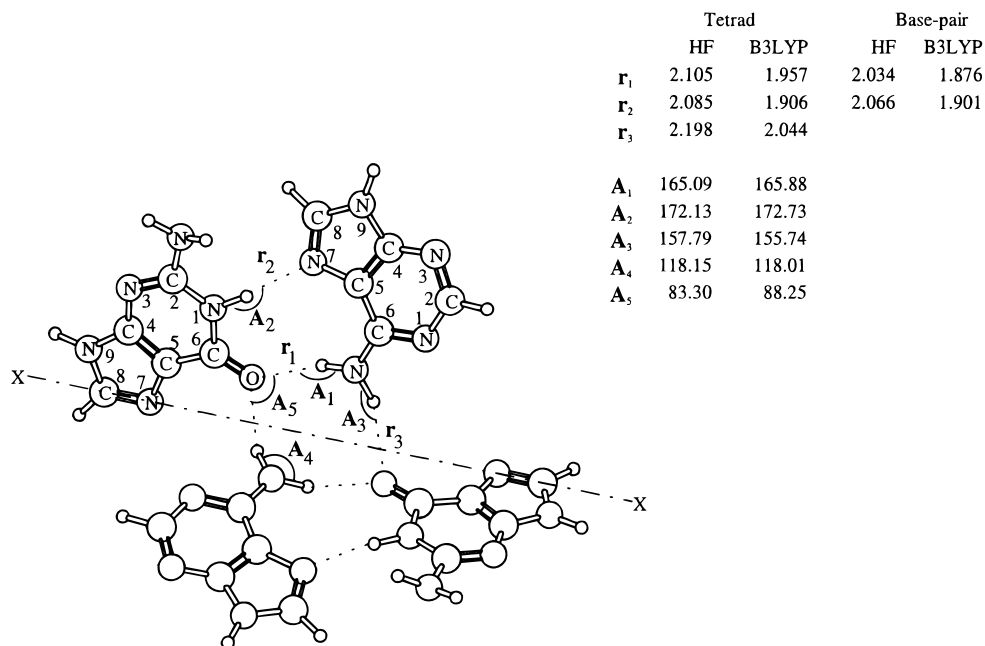


Figure 8. Fully optimized adenine-guanine-adenine-guanine tetrad (AGAG) structure. Atomic distances in angstroms and angles in degrees. X - X is the folding line. Base pair parameters are also listed for comparison. Basis set used in all the calculation is 6-311G(d,p).

an angle of 109° along the same axis. These two AG pairs are connected by the O6 of guanine and the protons linked to the N6 of the adenines. The lengths of the bifurcated H-bonds between the O6 of guanine and the H6 of the two adenines are 1.96 and 2.04 Å, respectively. The total binding energy of 29.4 kcal/mol of this tetrad is smaller than those of TATA tetrads, while the binding energy in the AG base pair is about 1 kcal/mol stronger than both Watson-Crick and Hoogsteen AT base pairs. Clearly, the weakness of the bifurcated H-bonds in the AGAG tetrad is due to the V-shape structure which distorts the O6-H6 bonding from their most favored directions. This V-shape structure of the tetrad results from the repulsive interactions between N1 of adenine and N7 of guanine, as can be seen in Figure 8. Consequently, compared to the two separated AG pairs, the AGAG tetrad has only 3.5 kcal/mol of stabilizing energy. Thus, the energy of the O6(G)···H(A) H-bond (r_3 in Figure 8) is about 1.75 kcal/mol which is consistent with that of the r_3 type in the TATA tetrads. A lack of r_4 type H-bonding in the AGAG tetrad decreases its stability and its folding angle. Although the molecular dynamics study suggests that the AGAG tetrad is favored in energy-minimized folded-back structures,¹⁴ the V-shape structure of the AGAG tetrad revealed in this study suggests that it cannot be stacked with the G-tetrads in the stem of the tetraplexes. Also, only 3.5 kcal/mol of stabilizing energy (compared to the two separated AG pair) implies that this tetrad structure may not be important in the tetraplexes. This result supports the conclusions of the previous experimental and theoretical studies.^{14,15}

Interestingly, the stabilization energies calculated at the DFT level are about 10 kcal/mol larger than the HF prediction (5–7 kcal/mol after the BSSE correction) for all three tetrads. The HF predicted relative stabilization energy of the AGAG tetrad is slightly larger than those of the TATA tetrads which is just the opposite in the DFT prediction. Considering the fact that there are two H-bonds less in the AGAG tetrad, this inverted result indicates that the H-bonding described at the HF level is much weaker than at the DFT level. Significant differences have been observed for the H-bond distances predicted by the DFT and HF methods. Generally, the bond distances inside the bases predicted at the HF level are slightly shorter (less than 0.03 Å)

compared to those obtained at the DFT level. However, the bifurcated hydrogen bond lengths are about 0.1–0.2 Å longer in the HF calculations than those in the DFT. The longer H-bond distances and the smaller stabilization energies of these tetrads suggest the importance of the electron correlation effects in forming bifurcated hydrogen bonds which govern the stabilization of the tetrads.

Conclusions

The following conclusions are revealed by the present quantum chemical studies.

(1) Both Hoogsteen- and Watson-Crick-type thymine-adenine-thymine-adenine tetrads are stable in the isolated form in which the Hoogsteen-type TATA tetrad is more stable than the Watson-Crick type. The stabilization energies of 32.7 and 30.4 kcal/mol confirm that the stabilization of the tetrads plays a key role in the four stranded helices.

(2) The energy of each bifurcated H-bond in the tetrads is about 8 kcal/mol for the planar structures and about 3 kcal/mol for the nonplanar structures. The bifurcated H-bonding is the main contribution to the formation and stabilization of the tetrad structures.

(3) The presence of a cation such as Na^+ , K^+ , or NH_4^+ in the system is expected to further stabilize the TATA tetrad in both forms. However, metal ions are unlikely to be stable in the center of the TATA tetrads.

(4) The V-shape structure of the AGAG tetrad and 3.5 kcal/mol of stabilizing energy (compared to the two separated AG pair) revealed in this study suggests that this tetrad structure may not be important in the tetraplexes.

Acknowledgment. This work was facilitated by the NIH Grant G12RR13459-21, by the Office of Naval Research Grant N00014-98-1-0592, and by the support of the Army High Performance Computing Research Center under the auspices of the Department of the Army, Army Research Laboratory cooperative agreement DAAH04-95-2-0003/Contract DAAH04-95-C-0008, the content of which does not necessarily reflect

the position or policy of the government, and no official endorsement should be inferred.

References and Notes

- (1) Gaillard, D.; Strauss, F. *Science* **1994**, *264*, 433.
- (2) Lebrun, A.; Laverny, R. *J. Biomol. Struct. Dyn.* **1995**, *13*, 459.
- (3) (a) Kang, C. H.; Zhang, X.; Ratliff, R.; Moyzis, R.; Rich, A. *Nature* **1992**, *356*, 126. (b) Laughlan, G.; Murchie, A. I. H.; Norman, D. G.; Moore, M. H.; Moody, P. C. E.; Lilley, D. M. J.; Luisi, B. *Science* **1994**, *265*, 520–524. (c) Phillips, K.; Dauter, Z.; Murchie, A. I. H.; Lilley, D. M. J.; Luisi, B. *J. Mol. Biol.* **1997**, *273*, 171.
- (4) (a) Smith, F. W.; Feigon, J. *Nature* **1992**, *356*, 164. (b) Smith, F. W.; Schultze, P.; Feigon, J. *Structure* **1995**, *3*, 997. Bouaziz, S.; Kettani, A.; Patel, D. J. *J. Mol. Biol.* **1998**, *282*, 637. (c) Hud, N. V.; Schultze, P.; Sklenar, V.; Feigon, J. *J. Mol. Biol.* **1999**, *285*, 233. (d) Deng, H.; Braunlin, N. V. *J. Mol. Biol.* **1996**, *255*, 476.
- (5) (a) Hardin, C. C.; Ross, W. S. *J. Am. Chem. Soc.* **1994**, *116*, 6080. (b) Strahan, G. D.; Keniry, M. A.; Shafer, R. H. *Biophys. J.* **1998**, *75*, 968. (c) Spackova, N.; Berger, I.; Sponer, J. *J. Am. Chem. Soc.* **1999**, *121*, 5519. (d) Bansal, M.; Ravikiran, M.; Chowdbury, S. In *Theoretical and Computational Chemistry, Vol. 8, Computational Molecular Biology*; Leszczynski, J., Ed.; Elsevier: New York, 1999; p 279.
- (6) Sarnam, M. H.; Luo, J.; Umamoto, K.; Yuan, R.; Sarma, R. H. *J. Biomol. Struct. Dyn.* **1992**, *9*, 1131.
- (7) Cheong, C.; Moore, P. B. *Biochemistry* **1992**, *31*, 8406.
- (8) Gu, J.; Leszczynski, J.; Bansal, M. *Chem. Phys. Lett.* **1999**, *311*, 209–214.
- (9) Metzger, S.; Lippert, B. *J. Am. Chem. Soc.* **1996**, *118*, 12467–12468.
- (10) Kettani, A.; Kumar, R. A.; Patel, D. J. *J. Mol. Biol.* **1995**, *254*, 638–656.
- (11) Darlow, J. M.; Leach, D. R. F. *J. Mol. Biol.* **1998**, *275*, 3–16.
- (12) Chernyi, A. A.; Lysov, Y. P.; Il'ychova, I. A.; Sibrov, A. S.; Shchyolkina, A. K.; Borisova, O. F.; Mamaeva, O. K.; Florentiev, V. L. *J. Biomol. Struct. Dyn.* **1990**, *8*, 513–527.
- (13) Balagurumoorthy, P.; Brahmachari, S. K. *J. Biol. Chem.* **1994**, *269*, 21858–21869.
- (14) Mohanty, D.; Bansal, M. *Biophys. J.* **1995**, *69*, 1046–1067.
- (15) Sundquist, W. I.; Klug, A. *Nature (London)* **1989**, *342*, 825.
- (16) Becke, A. D. *J. Chem. Phys.* **1993**, *98*, 5648.
- (17) Lee, C.; Yang, W.; Parr, R. G. *Phys. Rev. B* **1988**, *37*, 785.
- (18) Miehlich, B.; Savin, A.; Stoll, H.; Preuss, H. *Chem. Phys. Lett.* **1989**, *157*, 200.
- (19) Hehre, W. J.; Radom, L.; Schleyer, P. R.; Pople, J. A. *Ab initio Molecular Orbital Theory*; Wiley: New York, 1986.
- (20) Mebel, A. M.; Morokuma, K.; Lin, C. M. *J. Chem. Phys.* **1995**, *103*, 7414.
- (21) Johnson, B. G.; Gill, P. M. W.; Pople, J. A. *J. Chem. Phys.* **1993**, *98*, 5612.
- (22) Gu, J.; Leszczynski, J. *J. Phys. Chem.* **1999**, *103*, 577–584.
- (23) Sponer, J.; Leszczynski, J.; Hobza, P. *J. Phys. Chem.* **1996**, *100*, 1965–1974.
- (24) Frisch, M. J.; Trucks, G. W.; Schlegel, H. B.; Gill, P. M. W.; Johnson, B. G.; Robb, M. A.; Cheeseman, J. R.; Keith, T.; Petersson, G. A.; Montgomery, J. A.; Raghavachari, K.; Al-Laham, M. A.; Zakrzewski, V. G.; Ortiz, J. V.; Foresman, J. B.; Cioslowski, J.; Stefanov, B. B.; Nanayakkara, A.; Challacombe, M.; Peng, C. Y.; Ayala, P. Y.; Chen, W.; Wong, M. W.; Andres, J. L.; Replogle, E. S.; Gomperts, R.; Martin, R. L.; Fox, D. J.; Binkley, J. S.; Defrees, D. J.; Baker, J.; Stewart, J. P.; Head-Gordon, M.; Gonzalez, C.; Pople, J. A. *Gaussian 94*, revision D.3; Gaussian, Inc.: Pittsburgh, PA, 1995.
- (25) Boys, S. F.; Bernardi, F. *Mol. Phys.* **1970**, *19*, 553.